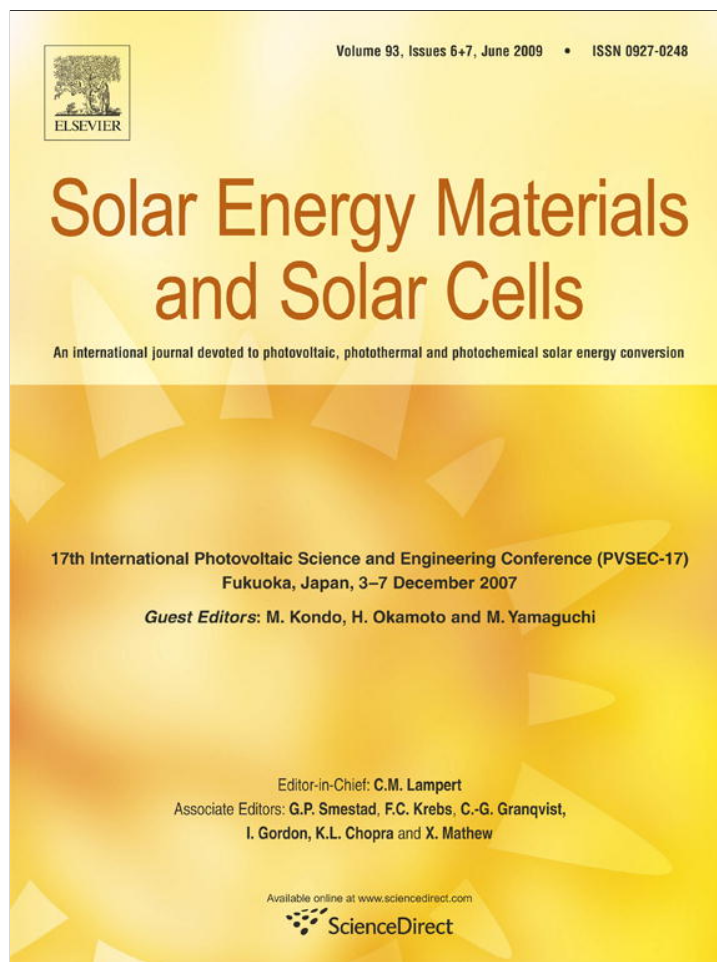


Provided for non-commercial research and education use.
Not for reproduction, distribution or commercial use.



This article appeared in a journal published by Elsevier. The attached copy is furnished to the author for internal non-commercial research and education use, including for instruction at the authors institution and sharing with colleagues.

Other uses, including reproduction and distribution, or selling or licensing copies, or posting to personal, institutional or third party websites are prohibited.

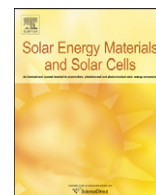
In most cases authors are permitted to post their version of the article (e.g. in Word or Tex form) to their personal website or institutional repository. Authors requiring further information regarding Elsevier's archiving and manuscript policies are encouraged to visit:

<http://www.elsevier.com/copyright>



Contents lists available at ScienceDirect

Solar Energy Materials & Solar Cells

journal homepage: www.elsevier.com/locate/solmat

Using scanning probe microscopy to study the effect of molecular weight of poly(3-hexylthiophene) on the performance of poly(3-hexylthiophene):TiO₂ nanorod photovoltaic devices

Ming-Chung Wu^a, Hsi-Hsing Lo^a, Hsueh-Chung Liao^a, Sharon Chen^a, Yun-Yue Lin^a, Wei-Che Yen^b, Tsung-Wei Zeng^a, Yang-Fang Chen^c, Chun-Wei Chen^a, Wei-Fang Su^{a,b,*}

^a Department of Materials Science and Engineering, National Taiwan University, 1, Roosevelt Road, Section 4, Taipei 106-17, Taiwan

^b Institute of Polymer Science and Engineering, National Taiwan University, Taipei 106-17, Taiwan

^c Department of Physics, National Taiwan University, Taipei 106-17, Taiwan

ARTICLE INFO

Article history:

Received 16 December 2007

Accepted 9 October 2008

Available online 19 December 2008

Keywords:

P3HT

TiO₂

Nanorods

Molecular weight

Heterojunction

ABSTRACT

We have studied the effect of polymer molecular weight on the performance of poly(3-hexylthiophene):TiO₂ hybrid photovoltaic device using atomic force microscopy (AFM) and scanning near-field optical microscopy (SNOM). The atomic force microscopic studies show the nanoscale morphology of the hybrid film changes from small domain size rod-like structure to large domain nodule-like structure with increasing the molecular weight of poly(3-hexylthiophene). The studies of SNOM of hybrid film reveal that the large domain structure of the high-molecular-weight P3HT hybrid film exhibits continuous absorption mapping as opposite to the discontinuous absorption mapping of the low-molecular-weight P3HT hybrid film. Both results suggest the improvement in device efficiency from high-molecular-weight P3HT is due to the formation of large domain structure with increased carrier mobility and light harvesting.

© 2008 Published by Elsevier B.V.

1. Introduction

Conjugated polymers are often utilized to fabricate large area, physically flexible and low-cost solar cells [1,2]. A basic requirement for efficient photovoltaic devices is for the free charge carriers produced upon photoexcitation of the photoactive material to be transported to the other electrode without recombining with oppositely charged carriers. Photovoltaic devices merely composed of conjugated polymers as the only active material have extremely low electron mobility, and thus, limited performance. Recent developments have shown that the use of interpenetrating electron donor–acceptor heterojunctions such as polymer:fullerene [2–4], polymer:polymer [5], and polymer:nanocrystal [6–8] can yield highly efficient photovoltaic conversions.

Titanium dioxide (TiO₂) nanocrystal is a promising electron accepting material in organic:inorganic hybrid photovoltaic applications. Several different conjugated polymers have been used in the polymer:TiO₂ solar cells such as poly [2-methoxy-5-(2'-ethyl-hexyloxy)-1,4-phenylene vinylene] (MEH-PPV) [9–12], MEH-PPV derivatives [13], poly[2-methoxy-5-(3',7'-dimethylocty-

loxy)-1,4-phenylene vinylene] (MDMO-PPV) [14], P3HT [7,15,16], and water-soluble polythiophene [17]. Most of the approaches to fabricate TiO₂ photovoltaic devices are infiltrating polymers into sintered TiO₂ nanoporous thin film.

In recent years, many researchers are studying the relationship between the field effect mobility and the molecular weight of a conducting polymer. McGehee and coworkers [18] have shown that when the molecular weight of P3HT increased, the detected field effect mobility increased as well. The mobility of P3HT is 1.7×10^{-6} and $9.4 \times 10^{-3} \text{ cm}^2 \text{ V}^{-1} \text{ s}^{-1}$ for its molecular weight at 3.2 and 36.5 kDa, respectively. They have used atomic force microscopy (AFM) to study the morphology of P3HT thin film made from different molecular weights. They have concluded that the large increase in mobility is due to the morphology difference between low-molecular-weight polymer and high-molecular-weight polymer. Scanning near-field optical microscopy (SNOM) is one of the high-resolution microscopic techniques that have been used to identify the relative distribution of polymers within a blend [19–23]. The SNOM is a particularly valuable analytical tool for the study of conjugated polymers [24] as many of the important processes pertinent to their applications involve the emission or absorption of photons. Furthermore, the SNOM permits spectroscopic measurements to be made on a surface with a high resolution less than 100 nm. Here, the SNOM was used

* Corresponding author. Tel./fax: +886 2 3366 4078.

E-mail address: suwf@ntu.edu.tw (W.-F. Su).

to observe the nanoscale optical properties of different molecular weights of poly(3-hexylthiophene) on the performance of poly(3-hexylthiophene):TiO₂ photovoltaic devices.

2. Experimental details

2.1. Synthesis of HT-HT poly(3-hexylthiophene) and characterization

The HT-HT poly(3-hexylthiophene) was synthesized according to literature with some modifications [25]. Typically, 2,5-dibromo-3-hexylthiophene (0.030 mol, 10 g) was added into a 500 ml three neck round bottom flask equipped with a 24/40 ground joint, a reflux condenser, and a magnetic stir-bar and was purged with dry nitrogen for 15 min. Totally 320 ml freshly distilled THF was transferred to the flask and the solution was stirred under dry nitrogen. The solution of tert-butylmagnesium chloride in diethyl ether (0.032 mol, 16 ml) was added via an airtight syringe and then heated in reflux for 1.5 h. The solution was allowed to cool toward room temperature followed by the addition of Ni(dppp)Cl₂, stirring at room temperature for 20 mins to 1 hr depending on the molecular weight. The solution was poured into methanol (500 ml). This action led to precipitation. The solid was collected in a cellulose extraction thimble and then washed with methanol in a Soxhlet apparatus. By changing the amount of Ni(dppp)Cl₂, the P3HT with different molecular weights (10, 30, and 66 kDa) was obtained. The polymer was dried in vacuum overnight and gathered as a dark purple material (60% yield).

2.2. Synthesis of TiO₂ nanorods and characterization

The controlled growth of the anatase titanium dioxide nanorods with a high aspect ratio was accomplished by hydrolyzing titanium tetraisopropoxide according to the literature with some modifications [12]. Typically, oleic acid (120 g, Aldrich, 90%) was stirred vigorously at 120 °C for 1 h in a three neck flask under Ar flow, then allowed to cool to 90 °C and maintained at the temperature. Titanium isopropoxide (17 mmol, Aldrich, 99.999%) was added into the flask. After stirring for 5 min, trimethylamine-N-oxide dehydrate (34 mmol, ACROS, 98%) in 17.0 ml water was rapidly injected. Trimethylamine-N-oxide dihydrate was used as a catalyst for polycondensation. This reaction was continued for 9 h to have a complete hydrolysis and crystallization process. Subsequently, the TiO₂ nanorod product was then obtained (4 nm in diameter, 20–40 nm in length). The nanorods were washed and precipitated using ethanol repeatedly to remove any residual surfactant. Finally, the TiO₂ nanorods were collected by centrifugation and then redispersed in chloroform. The crystalline structure of the TiO₂ nanorods was studied using X-ray diffraction (XRD) (Philips PW3040 with filtered Cu K α radiation ($\lambda = 1.540$ Å)). The analysis of the nanorods was performed using a JOEL JEM-1230 transmission electron microscope (TEM) operating at 120 kV or a 2000FX high-resolution transmission electron microscope (HRTEM) at 200 kV.

2.3. Fabrication of the nanostructure polymer blends/inorganic titania hybrid photovoltaic devices

The indium–tin-oxide (ITO)/poly(3,4-ethylenedioxythiophene)–poly(styrenesulfonate) (PEDOT:PSS)/poly(3-hexylthiophene):TiO₂ nanorods/Al device was fabricated in the following manner. An ITO glass substrate was ultrasonically cleaned in a series of organic solvents (ethanol, methanol, and acetone). A 60-nm-thick layer of PEDOT:PSS (Aldrich) was spin-casted onto the ITO substrate at 300 rpm for 10 s and 6000 rpm for 1 min

continuously. TiO₂ nanorods in pyridine and chloroform mixed solvent (weight ratios pyridine:chloroform = 2:7) and P3HT in chlorobenzene were thoroughly mixed and spin-casted on the top of the PEDOT:PSS layer (weight ratios TiO₂:P3HT = 53:47). The thickness of P3HT:TiO₂ nanorods film was 100 nm under 1000 rpm for a minute. Then, the 100 nm Al electrode was vacuum deposited on the hybrid layer. By inserting the TiO₂ nanorods thin film between the P3HT:TiO₂ nanorods hybrid and the Al electrode, an improved device with a configuration of ITO/PEDOT:PSS/P3HT:TiO₂ nanorods/Al was made.

2.4. Physical properties measurement of the nanostructure polymer blends/inorganic titania hybrid photovoltaic devices

Optical measurements were performed in the transmission mode using the scanning near-field optical microscopy (SNOM, WITec, AlphaSNOM, Germany) head with a special probe. The special probe with micro-fabricated cantilever SNOM sensors (aperture \sim 100 nm) exhibits a high transmission efficiency. Argon ion laser ($\lambda = 488$ nm), Nd:YAG laser ($\lambda = 532$ nm), and He–Ne laser ($\lambda = 632.8$ nm) with different wavelengths and output powers were employed as radiation sources. The transmitted light was collected with a 40 \times objective and detected with a single photon counting photomultiplier tube (PMT). For each line scan, 256 data points were taken with a line scan frequency of 0.5 Hz.

The film thickness was determined by an α -stepper (Veeco, Dektak 6M 24383). The film morphology was observed using AFM (Digital Instruments, Nanoscope III). The current–voltage (I – V) characterization (Keithley 2400 source meter) was performed under 10^{–3} Torr vacuum, with monochromatic illumination at a defined beam size (Oriel Inc.). The Air Mass (AM) 1.5 condition was measured using a calibrated solar simulator (Oriel Inc.) with irradiation intensity of 100 mW/cm². Once the power from the simulator was determined, a 400 nm cutoff filter was used to remove the UV light. The 80 nm films (P3HT or P3HT:TiO₂) were spin coated on a quartz substrate to obtain UV–visible absorption (Perkin–Elmer Lambda 35) and photoluminescence (PL) (Perkin–Elmer FS-55) measurements. The solution was prepared by dissolving 0.056 mg of P3HT in 1 ml of chlorobenzene.

3. Results and discussion

The TEM image of TiO₂ nanorods in the inset of Fig. 1 reveals that the dimensions of the TiO₂ nanorods are 20–30 nm in length and 4–5 nm in diameter. The HRTEM image of the TiO₂ nanorods is shown in Fig. 1. The above inset image shows the HRTEM image of TiO₂ nanorods crystallinity, and the corresponding selected-area diffraction pattern (SADP) of the TiO₂ nanorods is shown in the inset of Fig. 1. The d -spacings of this ring pattern are 3.54, 2.39, 1.90, and 1.69 Å from inner ring to outer ring. It can be indexed for (101), (004), (200), and (211) of the TiO₂ anatase phase, consistent with the XRD result. The filtered image from the square region is also shown, which indicates the growth direction of the TiO₂ nanorods is along the longitudinal [001] direction in the synthesized condition.

The polymers we used are similar in polydispersive index (PDI) and regiospecific ratio (RR), and the synthesizing process was the same for different molecular weight P3HT. We have assumed the effect of PDI, RR, and the ending groups of the polymer on its mobility is minimum and can be excluded because three polymers with the molecular weights in 10, 30, and 66 kDa, PDI < 1.5, and RR > 95% were used. We blended TiO₂ nanorods with different molecular weight P3HT and made into solar cell devices to study the effect of molecular weight on solar cell efficiency. The thickness of the hybrid film was all controlled at 120 nm. Fig. 2

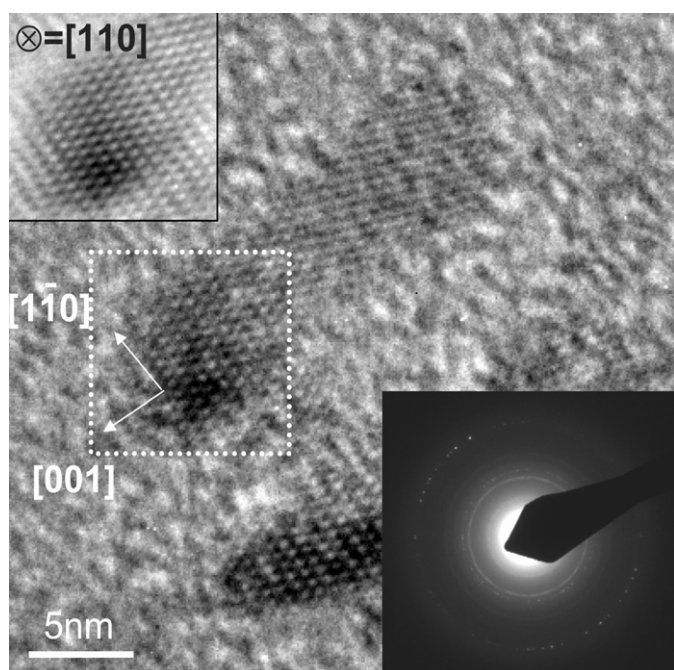


Fig. 1. Transmission electron microscope image of anatase TiO₂ nanorods.

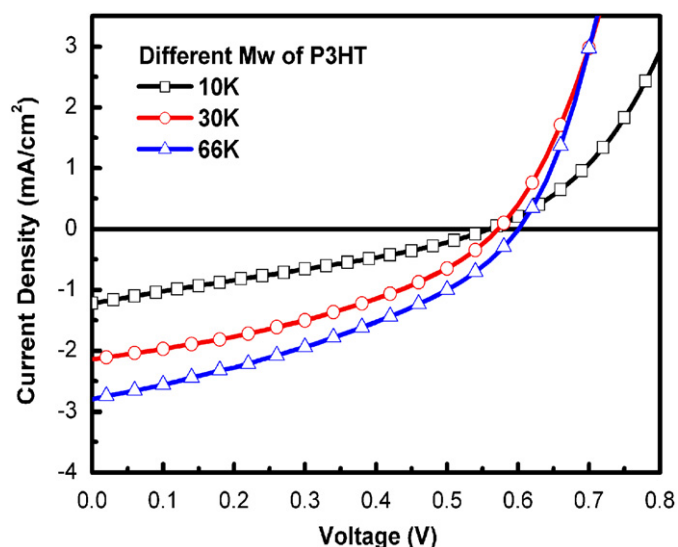


Fig. 2. The *I*–*V* characteristics under A.M. 1.5 illumination (100 mW/cm²) for photovoltaic device based on P3HT/TiO₂ nanorods (47/53 weight ratio) with different P3HT molecular weights.

is the *I*–*V* characteristic curves of the solar cells measured under A.M. 1.5 illumination. The data obtained from the *I*–*V* characteristic curves (*V*_{OC}, *I*_{SC}, FF, and the efficiency of the solar cell) are listed in Table 1. We can clearly observe an improvement in solar cell efficiency with increasing P3HT molecular weight. Why? We try to answer it using scanning near-field optical microscope (SNOM) and atomic force microscope.

The differences in molecular weights of a particular conducting polymer would result in different packing styles and conformations of its thin film and further affect its optical and electrical properties. The changes of the absorption peaks give the information of changes in the P3HT conformations. The absorption spectra of the solution and thin film of the P3HT with

Table 1
Performance of P3HT/TiO₂ nanorods hybrids solar cell under A.M. 1.5 illumination (100 mW/cm²) for different P3HT molecular weights

P3HT's MW (kDa)	<i>V</i> _{OC} (V)	<i>I</i> _{SC} (mA/cm ²)	FF (%)	Power conversion efficiency (%)
10	0.56	1.22	29.30	0.20
30	0.57	2.14	38.19	0.47
66	0.60	2.80	36.57	0.61

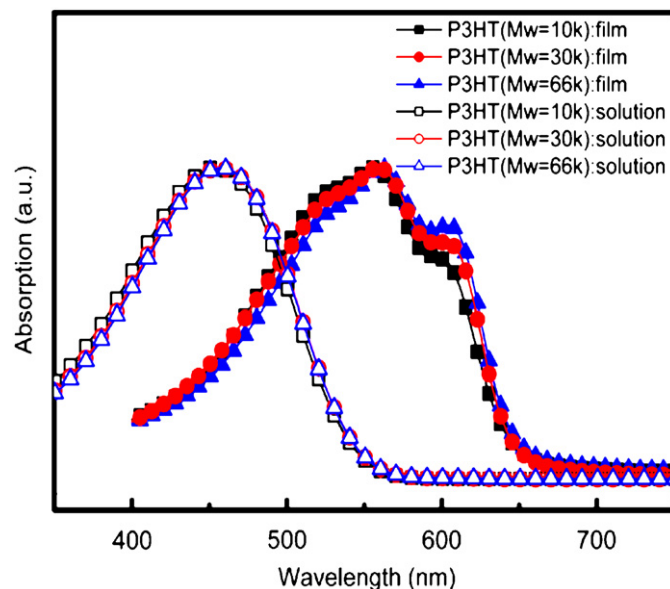


Fig. 3. Normalized absorption spectra of pure P3HT with different molecular weights: 10 kDa (–□–: solution; –■–: film), 30 kDa (–○–: solution; –●–: film), and 66 kDa (–△–: solution; –▲–: film).

different molecular weights are shown in Fig. 3. The absorption peaks show a trace of red shift in both solution and thin film samples. The conjugating length of the polymer increases with its molecular weight, so the extent of red shift in the absorption spectrum increases with its molecular weight. We have also observed a red shift in the absorption spectrum from solution sample to thin film sample. When the P3HT dissolves in the solvent, the repulsion force between repeating units arises due to steric effect. The alkyl side groups interact with the solvent and lead to a twist conformation of the P3HT backbone in the solution. On the other hand, when the P3HT is made into thin film, the interaction between polymer chains forms a π – π stacking, resulting in a lamellar structure. The ordered structured conformation of the P3HT thin film compared to solution P3HT facilitates the delocalization of π -electrons and an increase in conjugating length that results in a red shift of absorption spectrum.

It is important to investigate the absorption behavior of the hybrid film at nanoscale. We have used an SNOM to do the study. In the measurement, an SNOM probe with a hole of around 100 nm in diameter on the sharp end is placed into the near field of the investigated sample. The spatial resolution is then defined by the diameter of the hole. High-quality optical contrast images were obtained by this technique. In order to understand the absorption behavior under different laser wavelength excitation, the SNOM images of hybrid film sample made from 66 kDa P3HT and TiO₂ nanorods are shown in Fig. 4. Figs. 4a, c, and e are topographic images and Figs. 4b, d, and f are optical contrast

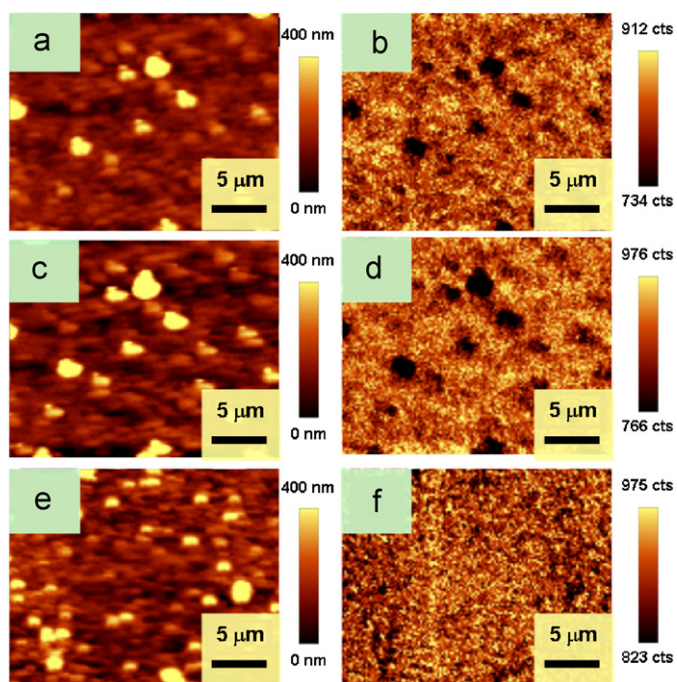


Fig. 4. Topography (a, c, and e) and optical contrast images (b, d, and f) of P3HT:TiO₂ samples with P3HT molecular weights of 66 kDa obtained in SNOM transmission mode using different monochromatic laser radiations. These three kinds of monochromatic laser are (a and b) argon ion laser ($\lambda = 488$ nm), (c and d) Nd:YAG laser ($\lambda = 532$ nm), and (e and f) He–Ne laser ($\lambda = 632.8$ nm).

images. Three kinds of monochromatic laser are argon ion laser ($\lambda = 488$ nm), Nd:YAG laser ($\lambda = 532$ nm), and He–Ne laser ($\lambda = 632.8$ nm) are used. Different contrast behaviors are observed for sample irradiated by different wavelength laser. Fig. 3(d) shows the highest absorption contrast at 532 nm laser excitation as compared with other laser excitation. The results are expected from the above absorption study, which shows the absorption maximum of the P3TH film is at 550 nm.

The SNOM was also used to study hybrid film. In order to decrease the PL behaviors of P3HT, the simultaneously topography and absorption measurements were measured using a He–Ne laser of 632.8 nm wavelength. The surface topography and absorption contrast images of three kinds of P3HT:TiO₂ samples with different P3HT molecular weights are shown in Fig. 5. The low-molecular-weight (10 kDa) sample exhibits coarse surface topography (Fig. 5a) and discontinuous absorption mapping behavior (Fig. 5b). The interchain stacking increases with increasing P3HT molecular weight that results in increasing smoothness of topography (Fig. 5c) and in becoming continuous absorption mapping at the corresponding region (Fig. 5d). The P3HT:TiO₂ sample with the highest molecular weight (66 kDa) exhibits smooth surface topography (Fig. 5d) and continuous absorption behavior (Fig. 5e) as compared with other samples. The results indicate the high-molecular-weight sample has a high light harvesting capability.

We have used high-resolution AFM to study the effect of polymer molecular weight on the nanoscale morphology of hybrid film. The results are shown in Fig. 6. The morphology and phase diagrams demonstrate that the rod-like structure is formed by low-molecular-weight P3HT while the high-molecular-weight P3HT tends to form small nodule-like structure. The nodule-like structure improves the transport of the charge carriers that has been reported [18]. The low-molecular-weight polymer has a great amount of grain boundaries that trap charges and slow

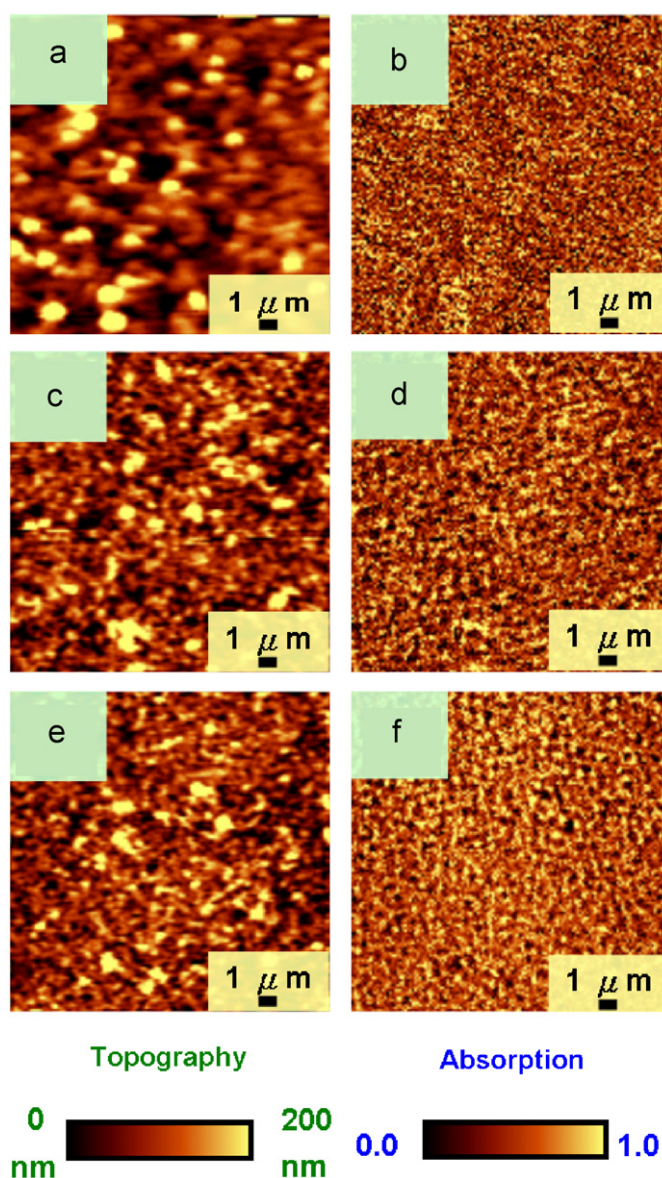


Fig. 5. Topography (a, c, and e) and optical contrast images (b, d, and f) of P3HT:TiO₂ samples with three kinds of P3HT molecular weights obtained in SNOM transmission mode using monochromatic laser radiation with 632.8 nm wavelengths. The P3HT molecular weight in P3HT:TiO₂ samples are (a and b) 10 kDa, (c and d) 30 kDa, and (e and f) 66 kDa.

down its transport. The results explain why the high-molecular-weight P3HT exhibits high solar cell efficiency.

4. Conclusions

We have fabricated the photovoltaic devices based on the bulk heterojunction of poly(3-hexylthiophene) (P3HT) and TiO₂ nanorods. The effect of molecular weight of P3HT on the performance of photovoltaic device was studied using scanning near-field optical microscopy (SNOM) and atomic force microscopy (AFM). The SNOM studies show a continuous absorption mapping for high-molecular-weight P3HT–TiO₂ hybrid film as opposite to the discontinuous absorption mapping for low-molecular-weight P3HT–TiO₂ hybrid film. The results suggest high light absorption for high-molecular-weight P3HT–TiO₂ hybrid film. The AFM studies reveal the large crystalline domain formation in the

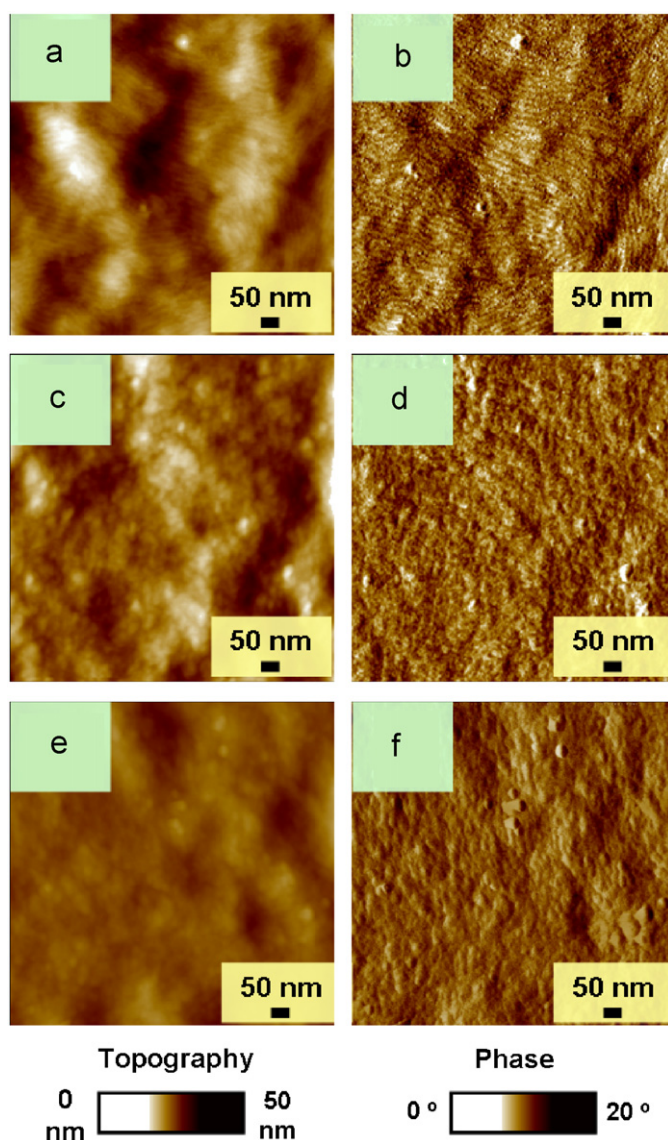


Fig. 6. Topography (a, c, and e) and phase images (b, d, and f) of P3HT:TiO₂ hybrid samples with three kinds of P3HT molecular weight obtained in AFM tapping mode, and the scan size is 2 μm × 2 μm. (a and b) The molecular weight of P3HT is 10 kDa. (c and d) The molecular weight of P3HT is 30 kDa. (e and f) The molecular weight of P3HT is 66 kDa.

high-molecular-weight P3HT–TiO₂ hybrid film that results in high carrier mobility. Therefore, the improvement in device efficiency by increasing the molecular weight of P3HT is due to the increase in both light harvesting and carrier mobility.

Acknowledgements

The financial support from the National Science Council of Taiwan (NSC-96-2628-E-002-017-MY3 and NSC 95-3114-P-002-003-MY3) is highly appreciated. The authors would also like to thank Prof. K.C. Cheng of National Taipei University of Technology, Prof. C.F. Lin, and Mr. Y.Y. Lin of National Taiwan University for helpful discussions.

References

- [1] W.U. Huynh, J.J. Dittmer, A.P. Alivisatos, Hybrid nanorod-polymer solar cells, *Science* 295 (2002) 2425.
- [2] W. Ma, C. Yang, X. Gong, K. Lee, A.J. Heeger, Thermally stable, efficient polymer solar cells with nanoscale control of the interpenetrating network morphology, *Adv. Funct. Mater.* 15 (2005) 1617.
- [3] S.E. Shaheen, C.J. Brabec, N.S. Sariciftci, F. Padiner, T. Fromherz, J.C. Hummelen, 2.5% efficient organic plastic solar cells, *Appl. Phys. Lett.* 78 (2001) 841.
- [4] X. Yang, J. Loos, S.C. Veenstra, W.J.H. Verhees, M.M. Wienk, J.M. Kroon, M.A.J. Michels, R.A.J. Janssen, Nanoscale morphology of high-performance polymer solar cells, *Nano Lett* 5 (2005) 579.
- [5] M. Granström, K. Petritsch, A.C. Arias, A. Lux, M.R. Andersson, R.H. Friend, Laminated fabrication of polymeric photovoltaic diodes, *Nature* 395 (1998) 257.
- [6] W.J.E. Beek, M.M. Wienk, M. Kemerink, X. Yang, R.A.J. Janssen, Hybrid zinc oxide conjugated polymer bulk heterojunction solar cells, *J. Phys. Chem. B* 109 (2005) 9505.
- [7] C.Y. Kwong, W.C.H. Choy, A.B. Djurišić, P.C. Chui, K.W. Cheng, W.K. Chan, Poly(3-hexylthiophene): TiO₂ nanocomposites for solar cell applications, *Nanotechnology* 15 (2004) 1156.
- [8] Y.Y. Lin, C.W. Chen, J. Chang, T.Y. Lin, I.S. Liu, W.F. Su, Exciton dissociation and migration in enhanced order conjugated polymer/nanoparticle hybrid materials, *Nanotechnology* 17 (2006) 1260.
- [9] Q. Fan, B. McQuillin, D.D.C. Bradley, S. Whitelegg, A.B. Seddon, A solid state solar cell using sol-gel processed material and a polymer, *Chem. Phys. Lett.* 347 (2000) 325.
- [10] H. Wang, C.C. Oey, A.B. Djurišić, K.K.Y. Man, W.K. Chan, M.H. Xie, Y.H. Leung, P.C. Chui, A. Pandey, J.M. Nunzi, Titania bicontinuous network structures for solar cell applications, *Appl. Phys. Lett.* 87 (2005) 023507.
- [11] Y.T. Lin, T.W. Zeng, W.Z. Lai, C.W. Chen, Y.Y. Lin, Y.S. Chang, W.F. Su, Efficient photoinduced charge transfer in TiO₂ nanorod/conjugated polymer hybrid materials, *Nanotechnology* 17 (2006) 5781.
- [12] T.W. Zeng, Y.Y. Lin, C.W. Chen, W.F. Su, C.H. Chen, S.C. Liou, H.Y. Huang, A large interconnecting network within hybrid MEH-PPV/TiO₂ nanorod photovoltaic devices, *Nanotechnology* 17 (2006) 5387.
- [13] R. Ravirajan, D.D.C. Bradley, J. Nelson, S.A. Haque, J.R. Durrant, H.J.P. Smith, J.M. Kroon, Efficient charge collection in hybrid polymer/TiO₂ solar cells using poly(ethylenedioxythiophene)/polystyrene sulphonate as hole collector, *Appl. Phys. Lett.* 86 (2005) 143101.
- [14] P.A. VanHal, M.M. Wienk, J.M. Kroon, W.J. Verhees, L.H. Sloof, W.J.H. Van Gennip, P. Jonkheijm, R.A.J. Janssen, Photoinduced electron transfer and photovoltaic response of a MDMO-PPV:TiO₂ bulk-heterojunction, *Adv. Mater.* 15 (2003) 118.
- [15] K.M. Coakley, M.D. McGehee, Photovoltaic cells made from conjugated polymers infiltrated into mesoporous titania, *Appl. Phys. Lett.* 83 (2003) 3380.
- [16] Y. Liu, M.A. Summers, C. Edder, J.M.J. Fréchet, M.D. McGehee, Using resonance energy transfer to improve exciton harvesting in organic-inorganic hybrid photovoltaic cells, *Adv. Mater.* 17 (2005) 2960.
- [17] Q. Qiao, J.T. McLeskey, Water-soluble polythiophene/nanocrystalline TiO₂ solar cells, *Appl. Phys. Lett.* 86 (2005) 153501.
- [18] R.J. Kline, M.D. McGehee, E.N. Kadnikova, J. Liu, J.M.J. Fréchet, Controlling the field-effect mobility of regioregular polythiophene by changing the molecular weight, *Adv. Mater.* 15 (2003) 1519.
- [19] A. Cadby, R. Dean, A.M. Fox, R.A.L. Jones, D.G. Lidzey, Mapping the fluorescence decay lifetime of a conjugated polymer in a phase-separated blend using a scanning near-field optical microscope, *Nano Lett* 5 (2005) 2232.
- [20] A. Cadby, R. Dean, R.A.L. Jones, D.G. Lidzey, Spontaneous emission control in micropillar cavities containing a fluorescent molecular dye, *Adv. Mater.* 18 (2006) 742.
- [21] A. Cadby, R. Dean, M. Stevenson, C. Elliot, R.A.L. Jones, A.M. Fox, D.G. Lidzey, Imaging the fluorescence decay lifetime of a conjugated-polymer blend by using a scanning near-field optical microscope, *Adv. Mater.* 19 (2007) 107.
- [22] E. Klimov, W. Li, X. Yang, G.G. Hoffmann, J. Loos, Scanning near-field and confocal Raman microscopic investigation of P3HT-PCBM systems for solar cell applications, *Macromolecules* 39 (2006) 4493.
- [23] C.R. McNeill, H. Frohne, J.L. Holdsworth, P.C. Dastoor, Near-field scanning photocurrent measurements of polyfluorene blend devices: directly correlating morphology with current generation, *Nano Lett* 4 (2004) 2503.
- [24] H. Aoki, M. Anryu, S. Ito, Synthesis and characterization of polyimides with low dielectric constants from aromatic dianhydrides and aromatic diamine containing phenylene ether unit, *Polymer* 46 (2005) 5896.
- [25] R.S. Loewe, S.M. Khersonsky, R.D. McCullough, A simple method to prepare head-to-tail coupled, regioregular poly(3-alkylthiophenes) using grignard metathesis, *Adv. Mater.* 11 (1999) 250.